Clays and Clay Minerals, Vol. 34, No. 5, 539–548, 1986.

CHEMISTRY OF DETRITAL BIOTITES AND THEIR PHYLLOSILICATE INTERGROWTHS IN SANDSTONES

ALA ADIN ALDAHAN AND SADOON MORAD

Department of Mineralogy and Petrology, Institute of Geology
Uppsala University, Box 555, S-75122 Uppsala, Sweden

Abstract—Microprobe analyses of optically homogeneous detrital biotites from sandstones of the Visingsö Group and the Dala Sandstone, Sweden, revealed a consistently low K content (generally <0.75 atom/formula unit) and variable amounts of Fe, Mg, Al, and Si. Electron probe profiles of some biotite grains indicated two major types of interstratification, one consisting of mainly illite layers and the other apparently consisting of chlorite layers. The layer thicknesses commonly ranged between 0.5 and 3 μm. Microprobe analyses of some thick (~5 μm) illitic layers indicated a phengitic composition, wherein the mica was relatively rich in octahederal Fe and Mg. The chloritic layers appeared to be Fe-Mg-rich and generally had octahederal totals of <6 atom/formula unit. Variations in the chemical composition of the biotite and some of the illite and chlorite were probably due to an uneven distribution of small amounts of the interstratified phases. The illite and chlorite layers were apparently formed by pseudomorphic replacement of detrital biotites, i.e., gradual replacement of one biotite layer by one layer(s) of illite and/or chlorite during diagenesis.

Key Words—Biotite, Chemical analysis, Chlorite, Diagenesis, Electron probe, Illite, Intergrowth.

INTRODUCTION

Most studies of the chemistry and alteration of biotite have been concerned with minerals in igneous and metamorphic rocks and in the weathering environment (e.g., Gilkes, 1973; Norrish, 1973; Gilkes and Suddhiprakarn, 1979; Craw *et al.*, 1982; Guidotti, 1984; Speer, 1984). Detrital biotites in sedimentary rocks have been largely ignored; however, the works of Kossovskaya *et al.* (1965) and, more recently, White *et al.* (1985) have been major contributions. In these studies it has been concluded that detrital biotites were diagenetically altered into chlorite, illite and/or kaolinite; some chemical analyses of these phases have been presented as well.

The identification of biotite is routinely based on microscopic observations; however, microprobe analyses of many grains that display optical properties similar to those of true biotite give chemical compositions deviating markedly from that of the pure mineral (see, e.g., Craw *et al.*, 1982; Mitchell and Taka, 1984; Morad, 1984). Such biotites are generally highly altered and have been called hydrobiotites (Foster, 1963; Craw *et al.*, 1982; Morad, 1984) or K-depleted biotites (White *et al.*, 1985).

The present paper reports systematic microprobe studies of such grains of altered biotite and discusses the relation between the composition of this detrital mica and the type of phyllosilicate intergrowths formed during diagenetic alteration. Diagenetic alteration of detrital biotite appears to be an important aspect in clay mineral genetic studies in sandstones.

MATERIALS AND METHODS

Sandstones from Upper and Middle Proterozoic formations, namely the Dala Sandstone and the Visingsö Group in central and southern Sweden, respectively, were studied. Details of the petrology and geology of those rocks were reported by Morad (1983), AlDahan (1985), and Morad and AlDahan (1986).

Microprobe analyses were made of 10 sandstone samples, rich in detrital biotite, from the Dala Sandstone and 10 from the Visingsö Group, using a Cambridge instrument operating at a 75° take-off angle, an accelerating voltage of 15 kV, and a sample current of 0.045–0.05 μA. A beam size of about 2 μm was obtained. Each analysis reported is the average of at least three analyses made on texturally and optically similar parts of the grain. The results were corrected for background, absorption, fluorescence, dead time, and atomic number effect using a computer program.

Microprobe analysis offers several advantages over bulk chemical analysis for the study of detrital biotite: (1) Individual biotite grains are commonly difficult to separate from lithified sediments, especially if they are present in small amounts. Therefore, chemical analyses of individual grains are easier to obtain by means of microprobe. (2) Biotite grains in the same sample may show different degrees of alteration (see, e.g., White *et al.*, 1985); hence, a bulk analysis of a purified biotite fraction is neither representative nor informative as to the paths of alteration. (3) Analyses of purified biotite fraction may reflect the iron and titanium oxides commonly found along cleavage planes. (4) Parts of many

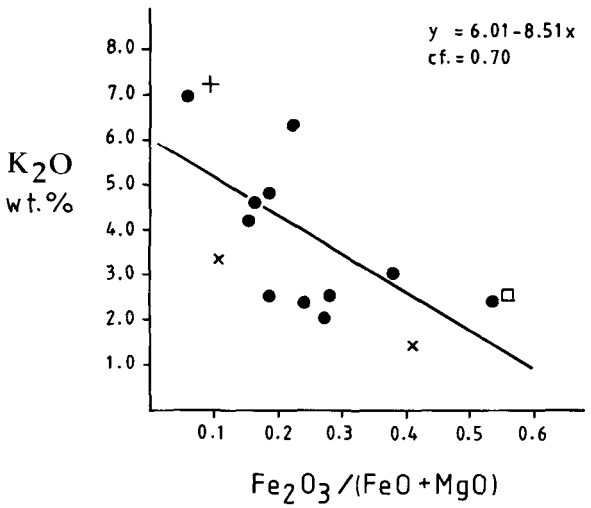

Figure 1. Plot of K_2O vs. $Fe_2O_3/(FeO + MgO)$ of altered biotite, □ = Walker (1949); × = Kossovskaya *et al.* (1965); ● = Foster (1963); + = Wilson (1970).

biotite grains are commonly altered to illite, chlorite, or kaolinite; hence, bulk analysis of purified fractions may give misleading results.

RESULTS AND INTERPRETATIONS

Structural formulae of biotite, illite, and chlorite

Although, as will be shown below, the chemical analyses of the biotites listed in Table 1 may not represent pure phases, an attempt was made to calculate the structural formulae from these data in order to compare these minerals on the basis of a mica-type unit-cell formula rather than on oxides alone. The analyses of biotites and illites were recalculated to unit-cell formulae on the basis of a trioctahedral mica (cf. Foster, 1960, 1963). Inasmuch as illite is a dioctahedral mica, all Si was assigned to the tetrahedral sheet together with enough Al to bring the total number of atoms to 4.00. The remaining Al and all Fe, Mg, and Ti were assigned to the octahedral sheet. All K was allocated to the interlayer sheet. The amounts of Mn and Na were very low (maximum of about 0.03 atom/formula unit) and therefore were not included in the biotite formula. Likewise Ti, Mn, Na, and Ca (maximum of about 0.05 atom/formula unit) were excluded from the illite formula. The chlorite formula was based on $O_{10}(OH)_8$ (Foster, 1962), and the elements were assigned to their respective sites as mentioned above, without, of course, interlayer cations (mainly K).

The Fe^{3+}/Fe^{2+} ratio in chlorite was estimated from wet-chemical analyses of two separated fractions of chloritized biotite (Morad and AlDahan, 1986). About 75% of the total iron was Fe^{2+}; thus a Fe^{3+}/Fe^{2+} ratio of 1/3 was used in Table 3. Although the amounts of Fe^{3+} and Fe^{2+} in the purified separations could reflect the presence of some Fe-bearing impurities, e.g., illitic minerals, hematite, or pyrite, the estimated ratio falls within the range of many chlorite analyses (e.g., Foster, 1962; Weaver and Pollard, 1973), which show about 70–85% of total iron as Fe^{2+}. For illites (Table 2), an Fe^{3+}/Fe^{2+} ratio of 7/1 was used (Merino and Ransom, 1982; AlDahan and Morad, 1986).

The Fe^{3+}/Fe^{2+} ratio for biotite was estimated by several methods. One method was to correlate the $Fe_2O_3/(FeO + MgO)$ with the K content of biotites following the conclusion of, e.g., Robert and Pedro (1969) and Ross and Rich (1974), who related the degree of Fe^{2+} oxidation in biotite to a specific stage of K depletion. For this purpose 11 biotite analyses presented by Foster (1963), one from Walker (1949), two from Kossovskaya *et al.* (1965), and one from Wilson (1970) were used to construct a regression line (Figure 1). The other two methods calculated total Fe as either only Fe^{2+} or as only Fe^{3+}. The formula of four biotites was constructed using these three methods (Table 4). To facilitate the comparison between results of these three methods and their maximum effect on variations in the structural formula of biotites, four analyses (from Table 1) having maximum iron content were chosen. By considering the Fe^{3+}/Fe^{2+} ratio obtained from the regression equation in Figure 1, a relatively good approximation between negative and positive charges was reached (Table 4, columns 2). The maximum deviation in the charge balance was obtained when Fe was calculated in only one state, i.e., either as Fe^{2+} or as Fe^{3+}, which suggests that appreciable amounts of both Fe^{2+} and Fe^{3+} are present in the biotite studied.

The approach described above to estimate the Fe^{3+}/Fe^{2+} ratio in biotite and the comparison made in Table 4 are reported here to illustrate a simple means of obtaining information about the state(s) of Fe in biotite, although the effects of impurities and submicroscopic interstratifications should be considered as well.

Chemistry of biotite, illite, and chlorite

Microprobe analyses of the biotites (Table 1) revealed two major types, both of which generally have a low K content. One type, however (Table 1, samples V_1–V_5 and D_1–D_5), is characterized by a relatively high content of interlayer K (0.38–0.75 atom/formula unit) and a low content of octahedral Fe (0.75–1.61 atom/formula unit). Generally, these biotites also have a total octahedral occupancy close to or less than the theoretical 3 atom/formula unit. Electron probe profiles of such grains (Figure 2) commonly show the presence of these two phases as interlayers <3 μm thick, which are rich in K but which contain different amounts of Fe and Mg, suggesting biotite and illite.

The second type of biotite (Table 1, samples V_6–V_{10} and D_6–D_{10}) is characterized by a relatively low content

Table 1. Microprobe analyses of detrital biotites.[1]

	V_1	V_2	V_3	V_4	V_5	Average	V_6	V_7	V_8	V_9	V_{10}	Average
SiO_2	33.1	33.4	33.1	32.4	34.1	33.22	28.1	29.7	28.1	27.5	28.3	28.34
Al_2O_3	15.6	14.1	13.9	16.1	16.2	15.18	16.4	16.6	16.6	16.5	18.9	17.00
FeO[2]	21.2	21.8	20.7	23.3	23.4	22.08	26.9	23.3	25.3	30.2	22.6	25.66
MgO	9.6	11.2	10.2	9.4	8.3	9.74	10.8	11.8	9.0	9.0	10.8	10.28
K_2O	6.0	7.3	6.5	4.8	6.1	6.14	2.2	2.5	3.0	2.3	2.0	2.40
TiO_2	1.8	2.9	3.6	1.2	1.6	2.22	1.3	1.4	2.1	0.6	1.9	1.46
MnO	0.43	0.45	0.12	0.40	0.40	0.36	0.38	0.30	0.43	0.40	0.26	0.35
Na_2O	0.21	0.10	0.04	0.21	0.00	0.12	0.09	0.06	0.23	0.00	0.06	0.09
Total	88.25	91.25	88.16	87.81	90.10	89.06	86.17	85.66	84.76	86.50	84.82	85.58
						Number of ions based on 22 negative charges						
Tet. Si	2.75	2.71	2.74	2.68	2.78	2.73	2.43	2.52	2.47	2.41	2.41	2.45
Al	1.25	1.29	1.26	1.32	1.22	1.27	1.57	1.48	1.53	1.59	1.59	1.55
Oct. Al	0.28	0.05	0.10	0.25	0.33	0.20	0.10	0.18	0.19	0.13	0.31	0.18
Fe	1.47	1.48	1.44	1.61	1.59	1.52	1.95	1.65	1.86	2.21	1.61	1.85
Mg	1.19	1.04	1.26	1.16	1.01	1.19	1.39	1.49	1.18	1.17	1.37	1.32
Ti	0.11	0.17	0.22	0.07	0.10	0.14	0.08	0.09	0.14	0.04	0.12	0.10
Σ Octahedral	3.05	2.74	3.02	3.09	3.03	3.05	3.51	3.41	3.37	3.55	3.41	3.45
Interlayer K	0.63	0.75	0.66	0.47	0.63	0.64	0.24	0.27	0.33	0.27	0.22	0.26
	D_1	D_2	D_3	D_4	D_5	Average	D_6	D_7	D_8	D_9	D_{10}	Average
SiO_2	32.3	37.9	41.5	37.4	36.9	37.20	33.2	30.9	29.5	34.9	28.5	31.40
Al_2O_3	22.9	25.1	29.5	19.3	19.7	23.30	21.7	19.1	16.9	20.9	18.5	19.42
FeO[2]	23.5	15.9	12.7	22.6	22.4	19.42	23.4	25.7	31.4	22.9	30.5	26.78
MgO	4.9	3.8	3.3	4.9	4.9	4.36	4.8	5.4	3.5	4.3	3.9	4.38
K_2O	4.1	4.7	6.0	3.9	3.8	4.50	3.0	3.0	3.0	2.4	2.2	2.68
TiO_2	0.24	0.08	0.08	0.30	0.30	0.20	0.05	0.20	0.90	0.60	0.40	0.43
MnO	0.45	0.44	0.20	0.38	0.39	0.37	0.46	0.60	0.42	0.00	0.00	0.29
Na_2O	0.12	0.09	0.14	0.00	0.00	0.07	0.08	0.00	0.04	0.06	0.00	0.04
Total	88.61	88.01	93.42	88.48	88.39	89.42	86.69	84.90	85.66	86.06	84.00	85.82
						Number of ions based on 22 negative charges						
Tet. Si	2.63	2.93	2.95	2.98	2.95	2.89	2.73	2.67	2.62	2.88	2.55	2.70
Al	1.37	1.07	1.05	1.02	1.05	1.11	1.27	1.33	1.38	1.12	1.45	1.30
Oct. Al	0.83	1.22	1.42	0.79	0.81	1.03	0.84	0.61	0.40	0.91	0.50	0.66
Fe	1.51	1.03	0.75	1.50	1.50	1.26	1.61	1.85	2.33	1.58	2.28	1.92
Mg	0.60	0.44	0.35	0.52	0.58	0.50	0.59	0.70	0.46	0.49	0.52	0.56
Ti	0.01	0.00	0.00	0.02	0.02	0.01	0.00	0.01	0.06	0.04	0.02	0.03
Σ Octahedral	2.95	2.69	2.52	2.89	2.91	2.80	3.04	3.17	3.25	3.02	3.32	3.17
Interlayer K	0.42	0.46	0.54	0.40	0.38	0.44	0.31	0.33	0.34	0.25	0.25	0.29

[1] V = Visingsö Group; D = Dala Sandstone.
[2] FeO represents total iron.

Table 2. Microprobe analyses of illite intergrown in detrital biotite.[1]

	V_1	V_2	V_3	V_4	V_5	V_6	V_7	V_8	Average	D_1	D_2	D_3	D_4	D_5	D_6	Average
SiO_2	51.3	52.3	48.3	50.6	49.7	51.3	52.2	47.6	50.41	44.3	44.9	43.9	43.7	44.1	45.1	44.33
Al_2O_3	25.4	28.4	25.9	30.9	26.5	28.1	30.8	28.7	28.09	22.6	33.8	25.5	25.5	32.4	38.8	29.76
FeO[2]	5.8	4.0	5.1	1.8	4.8	1.6	3.1	7.1	4.16	13.8	3.2	13.4	13.5	2.5	1.3	7.95
MgO	3.1	2.6	3.6	0.4	2.9	2.7	1.9	3.2	2.55	0.60	1.1	3.9	2.7	1.1	0.70	1.68
K_2O	4.2	5.1	7.4	6.4	4.3	3.5	6.4	4.5	5.22	6.7	4.6	3.6	8.6	7.6	9.8	6.82
TiO_2	0.20	0.41	0.22	0.19	0.23	0.28	0.24	0.46	0.28	0.21	0.32	0.66	0.23	0.41	0.27	0.35
MnO	0.10	0.21	0.16	0.00	0.04	0.19	0.18	0.31	0.15	0.13	0.11	0.13	0.14	0.00	0.12	0.10
Na_2O	0.23	0.12	0.10	0.00	0.04	0.18	0.15	0.00	0.10	0.06	0.08	0.05	0.00	0.00	0.24	0.07
CaO	0.16	0.00	0.7	0.10	0.04	0.16	0.14	0.12	0.09	0.02	0.07	0.04	0.00	0.04	0.00	0.03
Total	90.19	92.54	90.58	90.30	88.35	88.01	95.11	91.99	91.05	88.42	88.18	91.18	94.37	88.15	96.33	91.09
							Number of ions based on 22 negative charges									
Tet. Si	3.50	3.45	3.36	3.43	3.45	3.51	3.40	3.24	3.41	3.24	3.13	3.08	3.06	3.14	2.96	3.09
Al	0.50	0.55	0.64	0.57	0.55	0.49	0.60	0.76	0.59	0.76	0.87	0.92	0.94	0.86	1.04	0.91
Oct. Al	1.54	1.65	1.48	1.89	1.61	1.78	1.75	1.53	1.65	1.19	1.90	1.18	1.17	1.84	1.96	1.54
Fe^{3+}	0.26	0.17	0.23	0.07	0.24	0.06	0.13	0.35	0.20	0.74	0.1	0.68	0.67	0.12	0.05	0.39
Fe^{2+}	0.04	0.03	0.04	0.01	0.03	0.01	0.02	0.05	0.03	0.10	0.02	0.10	0.10	0.02	0.01	0.07
Mg	0.32	0.25	0.37	0.04	0.30	0.27	0.18	0.32	0.26	0.06	0.11	0.40	0.28	0.12	0.06	0.17
Σ Octahedral	2.16	2.10	2.12	2.01	2.17	2.12	2.08	2.25	2.14	2.09	2.19	2.36	2.22	2.10	2.08	2.17
Interlayer K	0.37	0.43	0.66	0.55	0.36	0.30	0.53	0.39	0.45	0.63	0.40	0.32	0.77	0.70	0.82	0.61

[1] V = Visingsö Group; D = Dala Sandstone.
[2] FeO represents total iron.

Table 3. Microprobe analyses of chlorite intergrown in detrital biotite.[1]

	V_1	V_2	V_3	V_4	V_5	V_6	V_7	Average	D_1	D_2	D_3	D_4	D_5	D_6	Average
SiO_2	29.7	28.9	29.1	28.7	30.2	30.9	30.2	29.67	25.4	26.9	31.8	32.5	24.8	20.6	27.00
Al_2O_3	17.6	15.2	20.1	16.5	17.6	19.7	17.6	17.76	17.7	18.7	17.8	17.1	21.7	15.7	18.12
FeO[2]	27.4	28.9	27.4	29.5	20.2	17.3	20.2	24.41	36.1	32.9	23.6	24.2	30.4	49.4	32.76
MgO	9.3	11.0	7.4	9.5	15.7	17.7	15.7	12.33	6.2	6.0	9.7	9.1	5.2	3.9	6.68
K_2O	0.23	0.64	0.82	0.49	0.48	0.36	0.39	0.49	0.50	0.91	0.86	0.90	0.80	0.83	0.80
TiO_2	0.04	0.04	0.11	0.00	0.26	0.00	0.02	0.07	0.10	0.11	0.10	0.22	0.77	0.56	0.31
MnO	0.31	0.33	0.46	0.44	0.47	0.39	0.38	0.39	0.20	0.23	0.32	0.28	0.38	0.41	0.30
Na_2O	0.07	0.17	0.00	0.00	0.00	0.05	0.15	0.06	0.00	0.00	0.08	0.00	0.05	0.12	0.04
CaO	0.00	0.08	0.04	0.00	0.00	0.04	0.21	0.05	0.00	0.00	0.03	0.04	0.02	0.00	0.02
Total	84.65	85.26	85.43	85.13	84.91	86.44	84.85	85.23	86.20	85.75	84.29	84.34	84.12	91.52	86.03
								Number of ions based on 28 negative charges							
Tet. Si	3.20	3.15	3.12	3.12	3.16	3.10	3.16	3.15	2.84	2.97	3.41	3.45	2.79	2.37	2.98
Al	0.80	0.85	0.88	0.88	0.84	0.90	0.84	0.85	1.16	1.03	0.59	0.55	1.21	1.63	1.02
Oct. Al	1.43	1.10	1.66	1.24	1.32	1.44	1.32	1.37	1.16	1.40	1.65	1.59	1.67	0.51	1.34
Fe^{2+}	1.85	1.99	1.85	2.03	1.34	1.10	1.33	1.62	2.54	2.29	1.59	1.63	2.17	3.59	2.27
Fe^{3+}	0.61	0.66	0.61	0.67	0.44	0.36	0.44	0.54	0.85	0.76	0.45	0.54	0.71	1.20	0.75
Mg	1.49	1.79	1.18	1.54	2.44	2.65	2.44	1.95	1.03	0.99	1.55	1.44	0.87	0.67	1.10
Σ Octahedral[3]	5.38	5.54	5.30	5.48	5.54	5.55	5.53	5.48	5.58	5.44	5.24	5.20	5.42	5.97	5.46

[1] V = Visingsö Group; D = Dala Sandstone.
[2] FeO represents total iron.
[3] Mn is 0.03–0.07 atom/formula unit.

Table 4. Calculation of formula of biotite from analyses in Table 1.[1]

	V_4			D_1			V_9			D_8		
	1	2	3	1	2	3	1	2	3	1	2	3
Fe_2O_3	0.00	8.8	25.9	0.00	6.7	26.1	0.00	18.2	33.5	0.00	12.2	34.9
FeO	23.3	15.4	0.00	23.5	17.5	0.00	30.2	13.8	0.00	31.4	20.4	0.00
Tet. Si	2.68	2.62	2.50	2.63	2.58	2.45	2.41	2.29	2.19	2.62	2.53	2.37
Al	1.32	1.38	1.50	1.37	1.42	1.55	1.59	1.63	1.55	1.38	1.47	1.60
Fe^{3+}								0.08	0.26			0.03
Oct. Al	0.25	0.25	0.05	0.83	0.74	0.50	0.13	0.00	0.00	0.40	0.24	0.00
Fe^{3+}	0.00	0.54	1.50	0.00	0.40	1.49	0.00	1.06	1.76	0.00	0.79	2.09
Fe^{2+}	1.61	1.04	0.00	1.51	1.17	0.00	2.21	0.96	0.00	2.33	1.46	0.00
Mg	1.16	1.13	1.06	0.60	0.58	0.55	1.17	1.11	1.07	0.46	0.45	0.42
Ti	0.07	0.07	0.07	0.01	0.01	0.01	0.04	0.04	0.03	0.06	0.05	0.05
Σ Octahedral	3.09	3.03	2.68	2.94	2.90	2.55	3.55	3.17	2.86	3.25	2.99	2.56
Interlayer K	0.47	0.39	0.37	0.42	0.41	0.40	0.27	0.24	0.23	0.34	0.33	0.32
Charge balance	−0.75	−0.39	−0.45	−0.62	−0.46	−0.44	−0.28	−0.23	−0.27	−0.36	−0.36	−0.32
Vacancy charge	−0.28	0.00	−0.64	−0.12	−0.20	−0.90	0.00	0.00	−0.28	0.00	−0.02	−0.88

[1] The analyses chosen represent maximum content of iron in illitized biotites (V_4 and D_1) and chloritized biotites (V_9 and D_8). The columns 1, 2, and 3 under each sample indicate the state(s) of iron used, thus in columns 1 all Fe is reported as Fe^{2+}; columns 2, Fe^{2+}/Fe^{3+} ratio is from regression equation in Figure 1; columns 3, all Fe is reported as Fe^{3+}.

of interlayer K (0.22–0.34 atom/formula unit) compared with the biotites described above, a high content of octahederal Fe (1.61–2.33 atom/formula unit), and a total octahedral occupancy greater than the theoretical 3 atom/formula unit. The Mg content is almost the same in both types of biotites.

Electron probe analyses of some grains showing characteristics of the second type of biotite (Figure 3) indicate a microinterlayering (<1–3 μm thick) of at least two phases. The chemical composition of the layers varies from K-rich to K-poor and mainly reflects a predominantly biotite and chlorite composition, as indicated by the high Fe and Mg contents of these layers. The small amounts of K in the K-poor (predominantly chloritic) layers may be due to submicroscopic biotite and/or illite interlayerings. Submicroscopic chlorite layers may also occur within the first type of biotite grains described above. Interstratifications of both biotite/chlorite and biotite/illite-muscovite on a finer scale and perhaps even on an Angström-unit scale are not out of the question (see, e.g., Lijima and Zhu, 1982; Veblen and Ferry, 1983).

The chemical analyses of the illite, occurring as 5-μm intergrowths in biotite (Table 2), suggest a phengitic composition and relatively high contents of octahedral Fe and Mg and low amounts of interlayer K. The octahedral occupancy is greater than the theoretical 2.00 atom/formula unit. Although illitic minerals (illite and illite/smectite) can accommodate some Fe and Mg in octahedral sites, the relatively high content of these elements (Table 2; e.g., analyses V_8, D_1, D_3, and D_4. See also Merino and Ransom, 1982, Table 1, analyses 3–5), particularly when they are coupled with low K, may possibly be due to submicroscopic interstratifications of biotite and/or chlorite.

The chemical analyses of the chlorite intergrowths, which occur as layers about 5-μm thick in biotite (Table 3) indicated a composition that varies between the chamosite and clinochlore of Bayliss (1975). These chlorites have large amounts of Fe and Mg in octahedral sites and octahedral totals of <6.0 atom/formula unit. Compared with the biotites (Table 1, samples V_6–V_{10} and D_6–D_{10}) the chlorites contain less tetrahedral Al and more octahedral Al and Mg. The small amounts of K reported in Table 3 and in many other analyses of chlorites (e.g., White *et al.*, 1985) are likely due to submicroscopic biotite and/or illite interstratifications.

Some compositional differences, particularly between the illites of the Dala Sandstone and the Visingsö Group (Table 2, samples D and V), are mainly due to different parageneses of the rock sequences (AlDahan and Morad, 1986). The Dala Sandstone has been diagenetically altered at higher conditions of temperature and pressure than the Visingsö Group, which has resulted in less expandable layers in the illite of the Dala

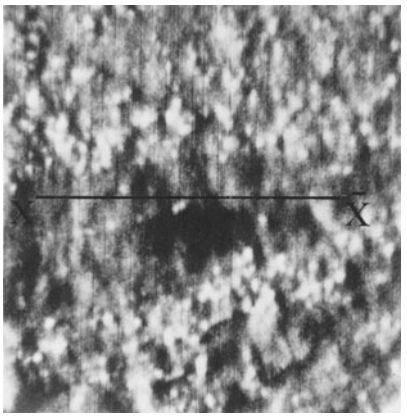

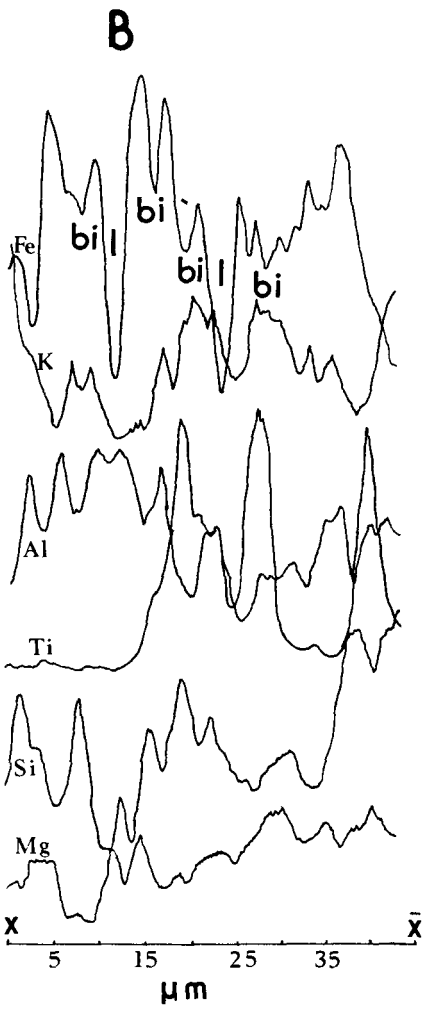

Figure 2. (A) Backscatter electronmicrograph of biotite grain showing the traverse probed in Figure 2B. (B) Microprobe profile showing the interlayering of mainly biotite (bi) and illite (I).

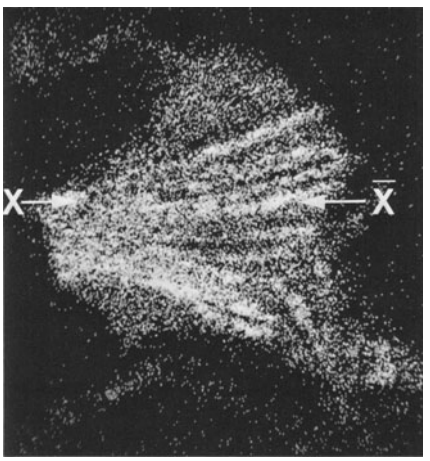

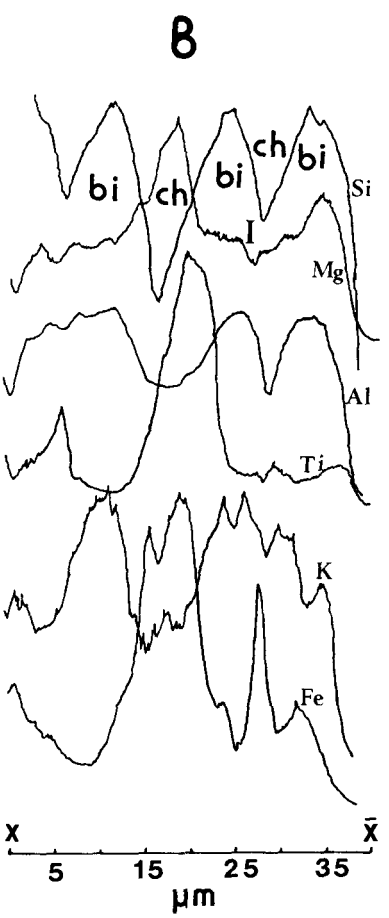

Figure 3. (A) X-ray photograph of Fe distribution in a biotite grain showing the interlayering of apparently biotite and chlorite and the traverse probed in Figure 3B. (B) Microprobe profile showing the interlayering of mainly biotite (bi) and chlorite (ch). I = minor illite.

https://doi.org/10.1346/CCMN.1986.0340507 Published online by Cambridge University Press

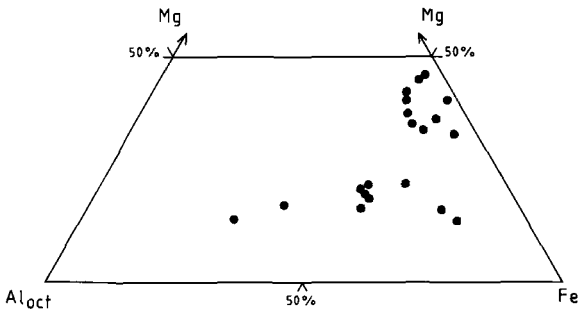

Figure 4. Compositional plot of biotites listed in Table 1 on a Mg-Fe-Al_{oct} triangle (See Foster, 1960).

relative to the Visingsö, as revealed by their K content (see averages in Table 2).

DISCUSSION AND CONCLUSIONS

Although the biotite analyses (Table 1) do not have the composition of true biotites, the triangular plot of the octahedral cations (Fe, Mg, Al; Figure 4) places them within or near the fields of Mg- and Fe^{2+}-biotites, which probably reflects their original composition, i.e., before alteration. Another feature of the biotites studied is the existence of a positive correlation between

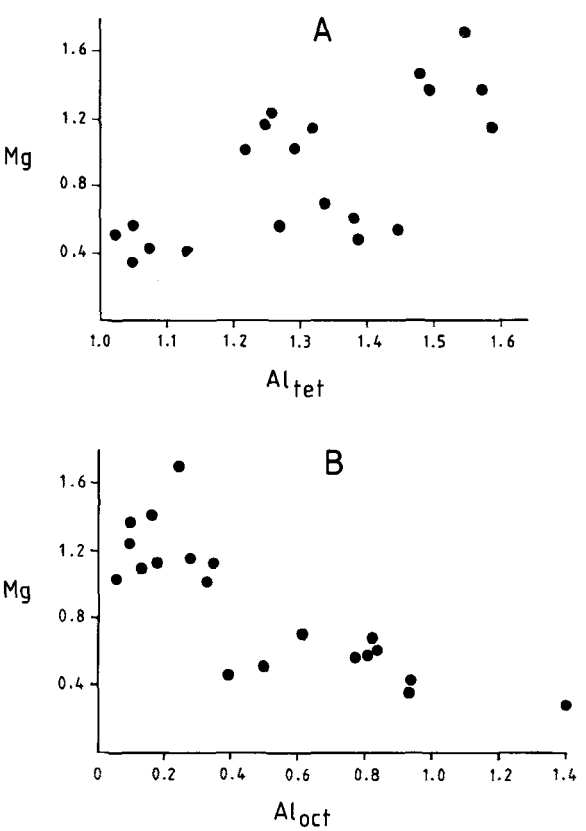

Figure 5. Mg vs. Al, tetrahedral (A) and octahedral (B) Al for biotites listed in Table 1.

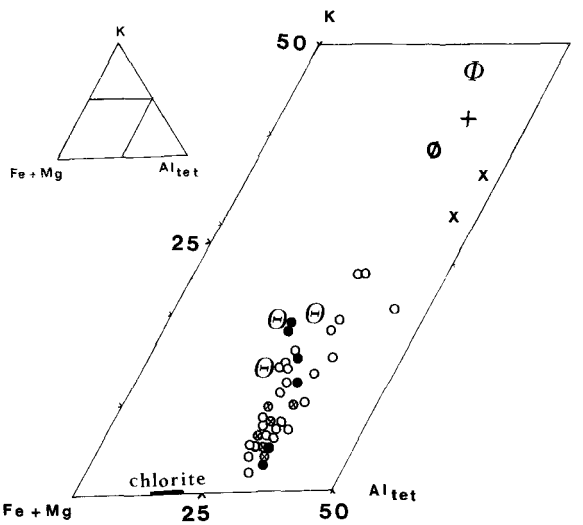

Figure 6. Compositional relation between biotite and replacement illite and chlorite. ○ = biotites (Table 1); ● = biotites (Craw *et al.*, 1982, analyses 3–5, 11, 12, and 16); ⊗ = biotites (White *et al.*, 1985, Table 4); × = illites (Table 2, averages); ϕ = illite (Craw *et al.*, 1982, average of analyses 6 and 7, Table 1); + = illite (White *et al.*, 1985, Table 4, analysis 1); Φ = muscovite and Θ = biotite (Deer *et al.*, 1966, Table 18, analyses 2, 5, 6, and 7).

Mg and Al_{tet} and a negative correlation between Mg and Al_{oct} (Figures 5A and 5B). These correlations suggest that substitution of Si for Al (most probably during gradual illitization of the biotite) was also accompanied by decrease of divalent cations in the octahedral sheet.

The biotite (Table 1), illite (Table 2), and chlorite (Table 3) analyses were plotted together with other analyses from the literature (Figures 6–8). Figure 6 shows the relation between K, (Fe + Mg), and Al_{tet} for biotites, illite-muscovite, and chlorite. On this diagram, the biotites show a spread in composition in a direction which is parallel to the line connecting the K/(Fe + Mg) ratios, i.e., along the directions of chlorite and illite-muscovite fields. This compositional trend probably reflects the amount of illite and/or chlorite intergrowths in biotite. The compositions of the two types of biotite described above, i.e., biotite interlayered with mainly illite and biotite interlayered with mainly chlorite, were plotted in Figues 7 and 8, respectively. The extent of intergrowth mentioned above can be assessed from these illustrations. In Figure 7 the amount of octahedral Al increases relative to (Fe + Mg) as the biotites change composition towards that of illite. In other words, the increase in the amount of illite interlayers appears to be correlated with increasing octahedral Al until pure illite is formed, which contains mainly Al in its octahedral sites. The relation between the proportions of chlorite intergrowths in biotite and the ratios of octahedral cations is less obvious (Figure 8) than the illitized biotite (Figure 7),

https://doi.org/10.1346/CCMN.1986.0340507 Published online by Cambridge University Press

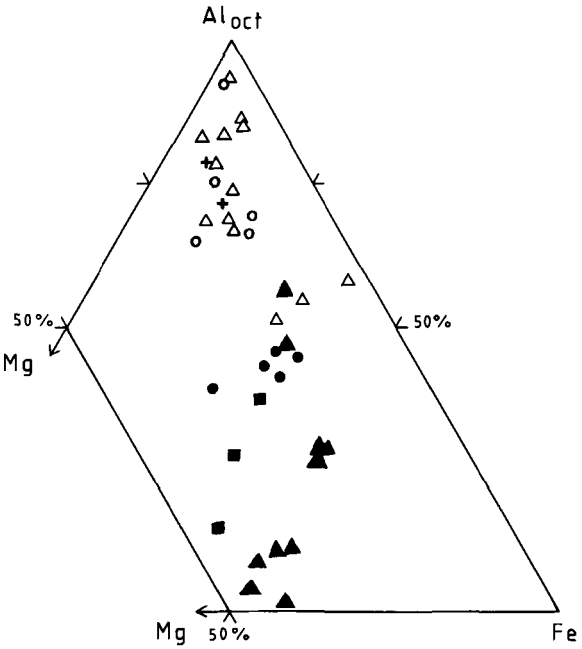

Figure 7. Compositional distribution of biotite and replacement illite. △ = illite (Table 2); ▲ = biotite (Table 1, analyses V_1–V_5 and D_1–D_5); ○ = illite and ● = biotite (Brøttum Formation, Morad, 1986); + = illite and ■ = biotite (Craw *et al.*, 1982, Table 1, analyses 3–7).

because both chlorite and biotite have variable amounts of Al, Fe, and Mg in the octahedral site; however, the biotite seems to change composition towards the Fe-Al_{oct} join as the amount of chlorite interlayers increases.

The above discussion suggests that biotites which deviate in their composition from true biotite should probably not be called hydrobiotites or K-depleted biotites (e.g., Craw *et al.*, 1982; Morad, 1984; Mitchell and Taka, 1984; White *et al.*, 1985). Instead, terms such as chloritized or illitized biotite (depending on the type of phyllosilicate intergrowths) are more suggestive of the mineralogical composition of these micas. The term hydrobiotite should be used, as indicated by Brindley *et al.* (1983), only for a regular 1:1 interstratification of biotite and vermiculite that gives a 24-Å superlattice spacing.

The intergrowth features of chlorite and illite, i.e., their proportions and composition, in the detrital biotites studied (see also Morad and AlDahan, 1986) vary from grain to grain in the same thin section. In some biotite grains, chlorite intergrowths dominate over illite and vice versa; in other grains only chlorite intergrowths are present. Such observations were also reported by other authors (e.g., White *et al.*, 1985). Furthermore, intergrowths of illite and/or chlorite with biotite were reported from rocks which had been affected by relatively high-grade diagenesis or early metamorphism (e.g., Craw *et al.*, 1982; White *et al.*, 1985; Morad, 1986). Although in such environments temperature-pressure conditions and solution chemistry appear to control the growth of minerals, the extent of each factor is not easy to evaluate. As mentioned above, however, it seems that the interlayering features, illite and chlorite, in biotite grains reflect the control of chemical-environmental variations on the scale of individual grains. Nevertheless, the chemical composition of individual illite-chlorite assemblages (i.e., within the same rock) could, to a large extent, reflect the effect of temperature-pressure conditions. For example, the variation in the chemical composition between the illites of the Visingsö Group and those of the Dala Sandstone were related to variation in the temperature and probably pressure, which have differently affected these units (AlDahan and Morad, 1986). Also the transformation of illite into muscovite and the increasing iron content in chlorites have been related to increasing temperature-pressure conditions (e.g., White *et al.*, 1985).

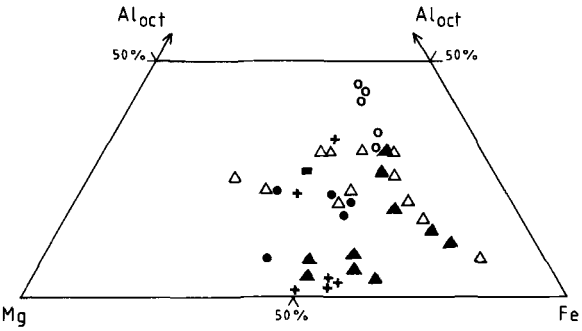

Figure 8. Compositional distribution of biotite and replacement chlorite. △ = chlorite (Table 3); ▲ = biotite (Table 1, analyses V_6–V_{10} and D_6–D_{10}); ○ = chlorite and ● = biotite (Brøttum Formation, Morad,1986); ■ = chlorite and + = biotite (White *et al.*, 1985, Tables 4 and 5, analyses 2–5, 7, 8).

The results of the present study and those of other authors (e.g., Craig *et al.*, 1982; White *et al.*, 1985) suggest that alteration of biotite during diagenesis is a potential source of K and/or (Fe + Mg) for the authigenesis of illites and chlorites.

ACKNOWLEDGMENTS

The microprobe analysis was performed at the Department of Mineralogy and Petrology (Uppsala) with the help of H. Harryson. K. Gløersen kindly typed the manuscript. The comments of S. W. Bailey, F. A. Mumpton, and another anonymous referee are gratefully acknowledged. S. Morad acknowledges the financial support from the Swedish Natural Science Research Council (NFR).

REFERENCES

AlDahan, A. A. (1985) Mineral diagenesis and petrology of the Dala Sandstone, central Sweden: *Bull. Geol. Inst. Uppsala* **12**, 1–48.

AlDahan, A. A. and Morad, S. (1986) Mineralogy and chemistry of diagenetic clay minerals in Proterozoic sandstones from Sweden: *Amer. J. Sci.* **286,** 29–80.

Bayliss, S. W. (1975) Nomenclature of the trioctahedral chlorites: *Can. Mineral.* **13,** 178–180.

Brindley, G. W., Zalba, P. E., and Bethke, C. M. (1983) Hydrobiotite, a regular 1:1 interstratification of biotite and vermiculite layers: *Amer. Mineral.* **68,** 420–425.

Craig, J., Fitches, W. R., and Maltman, A. J. (1982) Chlorite-mica stacks in low-strain rocks from central Wales: *Geol. Mag.* **119,** 243–256.

Craw, D., Coombs, D. C., and Kawachi, Y. (1982) Interlayered biotite-kaoline and other altered biotite, and their relevance to the biotite isograde in eastern Otago, New Zealand: *Mineral. Mag.* **45,** 79–85.

Deer, W. A., Howie, R. A., and Zussman, J. (1966) *An Introduction to the Rock-Forming Minerals:* Longmans, London, 528 pp.

Foster, M. D. (1960) Interpretation of the composition of trioctahedral micas: *Geol. Surv. Prof. Pap.* **354-B,** 49 pp.

Foster, M. D. (1962) Interpretation of the composition and a classification of the chlorites: *Geol. Surv. Prof. Pap.* **414-A,** 33 pp.

Foster, M. D. (1963) Interpretation of the composition of vermiculites and hydrobiotites: in *Clays and Clay Minerals, Proc. 10th Natl. Conf., Austin, Texas, 1961,* A. Swineford, ed., Pergamon Press, New York, 70–89.

Gilkes, R. J. (1973) The alteration products of potassium depleted oxybiotite: *Clays & Clay Minerals* **21,** 303–313.

Gilkes, R. J. and Suddhiprakarn, A. (1979) Biotite alteration in deeply weathered granite. I. Morphological, mineralogical and chemical properties: *Clays & Clay Minerals* **27,** 349–360.

Guidotti, C. V. (1984) Mica in metamorphic rocks: in *Micas, Reviews in Mineralogy 13,* S. W. Bailey, ed., Mineral. Soc. Amer., Washington, D.C., 375–456.

Iijima, S. and Zhu, J. (1982). Electron microscopy of a muscovite-biotite interface: *Amer. Mineral.* **67,** 1195–1205.

Kossovskaya, A. G., Drits, V. A., and Alexandrova, V. A. (1965) On trioctahedral mica in sedimentary rocks: in *Proc. Int. Clay Conf., Stockholm, 1963,* I. Th. Rosenqvist and P. G. Petersen, eds., Pergamon Press, Oxford, 147–169.

Merino, E. and Ransom, B. (1982) Free energies of formation of illite solid solutions and their compositional dependence: *Clays & Clay Minerals* **30,** 29–39.

Mitchell, J. G. and Taka, A. S. (1984) Potassium and argon loss patterns in weathered micas: implications for detrital mineral studies, with particular reference to the Triassic Palaeogeography of British Isles: *Sediment. Geol.* **39,** 27–52.

Morad, S. (1983) Diagenesis and geochemistry of the Visingsö Group (Upper Proterozoic), southern Sweden: a clue to the origin of color differentiation: *J. Sediment. Petrol.* **53,** 51–65.

Morad, S. (1984) Diagenetic matrix in Proterozoic greywacke sandstones from Sweden: *J. Sediment. Petrol.* **54,** 1157–1168.

Morad, S. (1986) Mica-chlorite intergrowths in very low-grade metamorphosed sedimentary rocks from Norway: *Neues Jahrb. Mineral.* (in press).

Morad, S. and AlDahan, A. A. (1986) Diagenetic alteration of biotite in Proterozoic sedimentary rocks from Sweden: *Sediment. Geol.* **47,** 95–107.

Norrish, K. (1973) Factors in the weathering of mica to vermiculite: in *Proc. Internat. Clay Conf., Madrid, 1972,* J. M. Serratosa, ed., Div. de Ciencias, Madrid, 417–432.

Robert, M. and Pedro, G. (1969) Etude des relations entre les phénomènes d'oxydation et l'aptitude à l'ouverture dans les micas trioctaédriques: in *Proc. Internat. Clay Conf., Tokyo, 1969, Vol. 1,* L. Heller, ed., Israel Universities Press, Jerusalem, 455–473.

Ross, G. J. and Rich, C. I. (1974) Effect of oxidation and reduction on potassium exchange of biotite: *Clays & Clay Minerals* **22,** 355–360.

Speer, J. A. (1984) Micas in igneous rocks: in *Mica, Reviews in Mineralogy 13,* S. W. Bailey, ed., Mineralogical Society of America, Washington, D.C., 299–356.

Veblen, D. R. and Ferry, J. M. (1983) A TEM study of the biotite-chlorite reaction and comparison with petrologic observations: *Amer. Mineral.* **68,** 1160–1168.

Walker, G. F. (1949) The decomposition of biotite in the soil: *Mineral. Mag.* **28,** 693–703.

Weaver, C. E. and Pollard, L. D. (1973) *The Chemistry of Clay Minerals:* Elsevier, New York, p. 213.

White, S. H., Huggett, J. M., and Shaw, H. F. (1985) Electron-optical studies of phyllosilicate intergrowths in sedimentary and metamorphic rocks: *Mineral. Mag.* **49,** 413–423.

Wilson, M. J. (1970) A study of weathering in a soil derived from a biotite-hornblende rock. I. Weathering of biotite: *Clay Miner.* **8,** 291–303.

(Received 3 September 1985; accepted 16 April 1986; Ms. 1515)